metals

MDPI

Article

The Effect of Mo and Dispersoids on Microstructure, Sintering Behavior, and Mechanical Properties of W-Mo-Ni-Fe-Co Heavy Tungsten Alloys

Chun-Liang Chen [1,*] and Sutrisna [1,2]

[1] Department of Materials Science & Engineering, National Dong Hwa University, Shou-Feng, Hualien 97401, Taiwan

[2] Department of Mechanical Engineering, Sekolah Tinggi Teknologi Nasional, Yogyakarta 55281, Indonesia; 810422003@gms.ndhu.edu.tw

* Correspondence: chunliang@gms.ndhu.edu.tw; Tel.: +886-3-8903205

Received: 28 December 2018; Accepted: 18 January 2019; Published: 22 January 2019

Abstract: W-Mo-Ni-Fe-Co heavy tungsten alloys were fabricated by mechanical alloying. The effects of Mo and oxide dipsersoids on the characteristics and properties of the model alloys were investigated. In this study, the W-Mo matrix and γ-Ni(Fe,Co) binder phase were further synthesized with Y_2O_3 by a secondary ball milling method. The results suggest that the microstructure and sintering behavior of the model alloys are strongly influenced by the dispersed oxide particles. The model alloys with the Y_2O_3 addition demonstrate grain refinement and uniform microstructure. The dispersed particles could act as an inhibitor for diffusion of tungsten atoms and grain growth, promoting the formation of solid state during sintering. Consequently, good densification, high hardness, and elastic modulus of alloys can be achieved.

Keywords: heavy tungsten alloy; mechanical alloying; sintering

1. Introduction

Tungsten heavy alloys (WHAs) are promising materials for a wide range of applications in medical, military, and aerospace industries, such as radiation shields, kinetic energy penetrators, and counterbalance weights [1,2], due to their superior properties, such as high strength, high density, high radiation absorption, and good wear resistance [2–4]. In WHAs, nickel, iron, copper, and cobalt elements are commonly added to a tungsten matrix and serve as a binder phase, which helps in providing ductility to the materials [5–7]. In recent years, oxide dispersion strengthened (ODS) tungsten heavy alloys have attracted attention as potential high temperature structural materials [8–12]. The nano-oxide dispersed particles can be intentionally introduced or formed in-situ by mechanical alloying, which can further enhance high temperature strength and ductility of materials [6]. The ODS WHAs are normally produced by mechanical alloying, which is a solid-state powder metallurgy processing technique that involves repeated cold welding, fracturing and rewelding of powder particles. During mechanical alloying, some parameters should be taken into account to prevent material contamination, such as grinding media materials, the process control agent (PCA), and the milling atmosphere [9,10].

In our previous research [8–12], W-Ni-Fe and W-Ni-Co alloys fabricated by mechanical alloying have been investigated. The change of the Ni/Fe or Ni/Co ratios can result in the formation of embrittling intermetallics and the solid to liquid phase transition during sintering [10,12]. Furthermore, it has been reported that the addition of molybdenum to W–Ni–Fe alloys by mechanical alloying can enhance the hardness, yield strength, and ultimate tensile strength of the

materials [13,14]. Additionally, the presence of cobalt in WHAs increases interfacial strength between the binder phase and tungsten matrix, which can improve both strength and ductility [15].

In this study, new ODS heavy tungsten alloys based on W-Mo-Ni-Fe-Co have been developed. The molybdenum within the alloys can provide solid solution strengthening of the tungsten matrix phase. Therefore, a two-stage ball milling procedure is introduced to synthesize the model alloys. The W-Mo matrix phase and Ni-Fe-Co binder phase are pre-milled individually, and then the two phases are secondarily milled with Y_2O_3 dispersed particles for a long period of time. The focus of this study is to investigate the effects of the addition of Mo and dispersoids on microstructural evolution and the mechanical properties of W-Mo-Ni-Fe-Co alloys. Additionally, it is important to understand how nano-oxide particles and secondary ball milling influence the characteristics and sintering behavior of the model alloys. Finally, synthesis of new tungsten-based ODS alloys can achieve refined microstructure and improved mechanical properties.

2. Materials and Methods

The four W-Mo-Ni-Fe-Co model alloys dispersed with Y_2O_3 and possessing variable Mo contents synthesized by mechanical alloying were studied and named W3Mo, W12Mo, W3Mo-YO, and W12Mo-YO. The detail of each model alloy can be seen in Table 1. The raw materials used in this study were W, Mo, Ni, Fe, and Co elemental powders with a purity of 99.9% and particle sizes from 20 μm to 50 μm (supplied by Gredmann Group, Taiwan). Nano-oxide particles of Y_2O_3 (~20 nm in size) were introduced for dispersion strengthening. The model alloys were produced by a two-stage milling procedure. In the first stage of ball milling, the W-Mo matrix powders and Ni-Fe-Co binder powders were pre-milled for 24 h, respectively. The matrix and binder phase powders were then secondarily ball milled with Y_2O_3 for 4h, 8 h, 16 h, and 24 h.

Mechanical alloying was carried out in a planetary ball mill (Retsch PM100, Retsch GmbH, Haan, Germany) with 350 rpm under an argon atmosphere for different milling times. A tungsten carbide grinding medium with a ball to powder ratio of 10:1 was used in this work. The mechanically alloyed powders were consolidated into green compacts with a pressure of 210 MPa and then sintered at 1723 K for 60 min under a mixed hydrogen-argon atmosphere. Microstructure characterization of the milled powders and sintered model alloys was carried out using an X'Pert PRO X-ray diffractometer (XRD) (PANalytical, Almelo, Netherlands), an Olympus BX41M-LED light microscope (Olympus, Tokyo, Japan), and a Hitachi-4700 scanning electron microscope (SEM) with energy-dispersive X-ray spectroscopy (EDS). The relative densities of the sintered alloys were determined by the Archimedes method, using water immersion. The Vickers hardness measurements were performed at room temperature using a 1kg load for 15 seconds. Nanoindentation measurements (MTS Nanoindenter XP, MTS Systems Corporation, Eden Prairie, MN, USA) were conducted to obtain the hardness and elastic modulus using the continuous stiffness measurement (CSM) method.

Table 1. The composition of the W-Mo-Ni-Fe-Co model alloys (wt.%).

Model alloys	W	Mo	Ni	Fe	Co	Y_2O_3
W3Mo	Bal.	3	7	1.5	1.5	-
W12Mo	Bal.	12	7	1.5	1.5	-
W3Mo-YO	Bal.	3	7	1.5	1.5	2
W12Mo-YO	Bal.	12	7	1.5	1.5	2

3. Results

3.1. Characterization of the Milled Powders

Figure 1 shows the XRD spectra of the Ni-Fe-Co powders as a function of milling time. The strong diffraction peaks corresponding to (111), (200), (220), (311), and (222) reflections of the nickel phase were observed. By increasing the milling time, the characteristic peaks of Fe and Co disappeared, suggesting that Fe and Co atoms dissolved into the Ni crystalline lattice, promoting the

formation of a solid solution of γ-Ni(Fe,Co) during ball milling. It should be noted that the nickel carbide phase was detected, corresponding to contamination generated by the mechanical alloying process after the long grinding time. The Ni peaks slightly shifting with increasing milling time were observed from the XRD spectra, indicating the formation of a solid solution of γ-Ni(Fe,Co) due to the expansion of the lattice parameters.

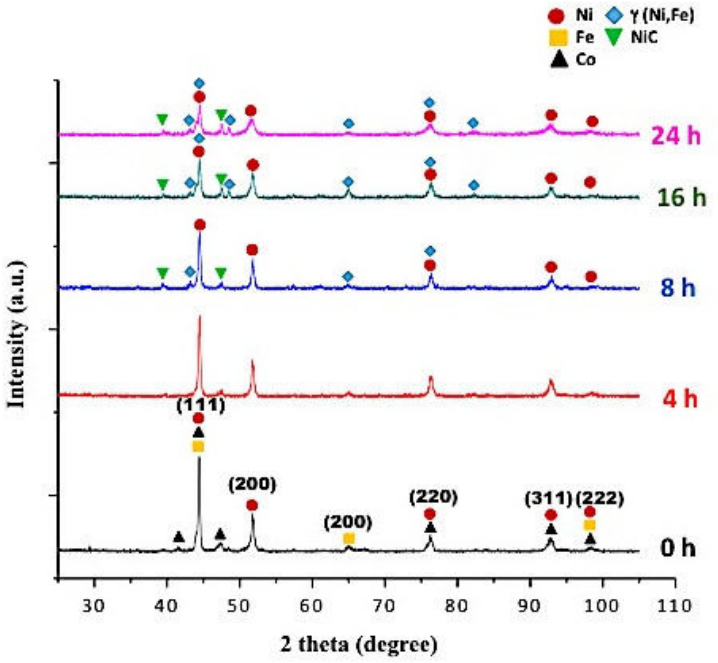

Figure 1. X-ray diffraction (XRD) spectra of the Ni-Fe-Co powders milled for 0 h, 4 h, 8 h, 16 h, and 24 h.

In this study, the W-Mo matrix powders were pre-milled for 24 h. The W-Mo matrix and γ-Ni(Fe,Co) binder phase were further milled with nano-Y_2O_3 oxides by secondary ball milling. Figure 2a shows the XRD spectra of the W-Mo/γ-Ni(Fe,Co) powders as a function of milling time. It can be seen clearly that the peak of the binder phase γ-Ni(Fe,Co) disappeared after 16 h of milling, which suggested diffusion of the binder phase into the W crystalline lattice and caused the formation of a solid solution during mechanical alloying. Furthermore, the intensities of the W peaks gradually decreased with increasing milling time. It is a well-known fact that peak broadening occurs when heavy deformation is created by mechanical alloying and causes a number of crystal defects, such as dislocations, vacancies, twin faults, and stacking faults [11]. The results can be associated with the evolution of crystallite size and lattice strain as a function of milling time (see Figure 2b). The crystallite size of the milled powders decreased from 24.24 to 12.78 nm with increasing milling time. This indicates that the refinement of the grain size and an increase of internal strain were promoted by the increase of milling time. It should be noted that the existence of structural defects can promote the diffusivity of the binder γ-Ni(Fe,Co) phase into the W-Mo matrix.

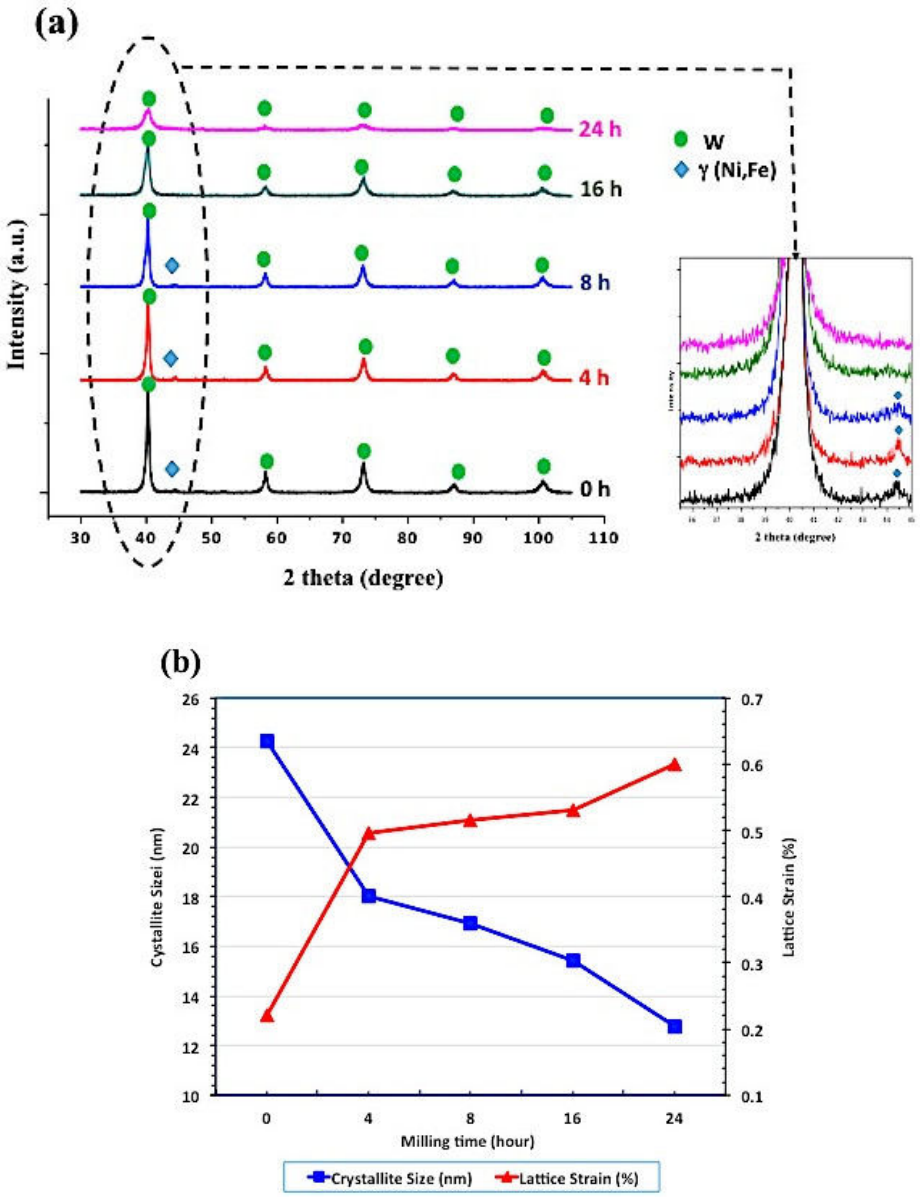

Figure 2. (a) XRD spectra of the W-Mo matrix/γ-Ni(Fe,Co) binder powders milled for 0 h, 4 h, 8 h, 16 h, and 24 h; **(b)** crystallite size and lattice distortion of the W-Mo matrix/γ-Ni(Fe,Co) binder powders milled as a function of milling time.

3.2. *Characterization of the Sintered Model Alloys*

3.2.1. Optical Microscope

Figure 3 shows optical images of the sintered W-Mo-Ni-Fe-Co model alloys milled for 24 h. The microstructure of the W3Mo model alloy (Figure 3a) illustrates the tungsten matrix has a large spherical grain size and is interconnected with the γ-Ni(Fe,Co) binder phase. Moreover, the W12Mo model alloy has a similar microstructure to the W3Mo sample; however, a number of pores were found in the sample with more Mo (Figure 3b). The large spherical grain structure observed in the model alloys indicates the formation of a liquid phase during sintering. On the other hand, the model alloys dispersed with Y_2O_3 oxides show significant grain refinement and uniform microstructure, corresponding to the formation of a solid phase during sintering (Figure 3b,d). Therefore, it is believed that the addition of Y_2O_3 plays an important role in determining the sintering behavior of the model alloys. This will be further discussed in the following section.

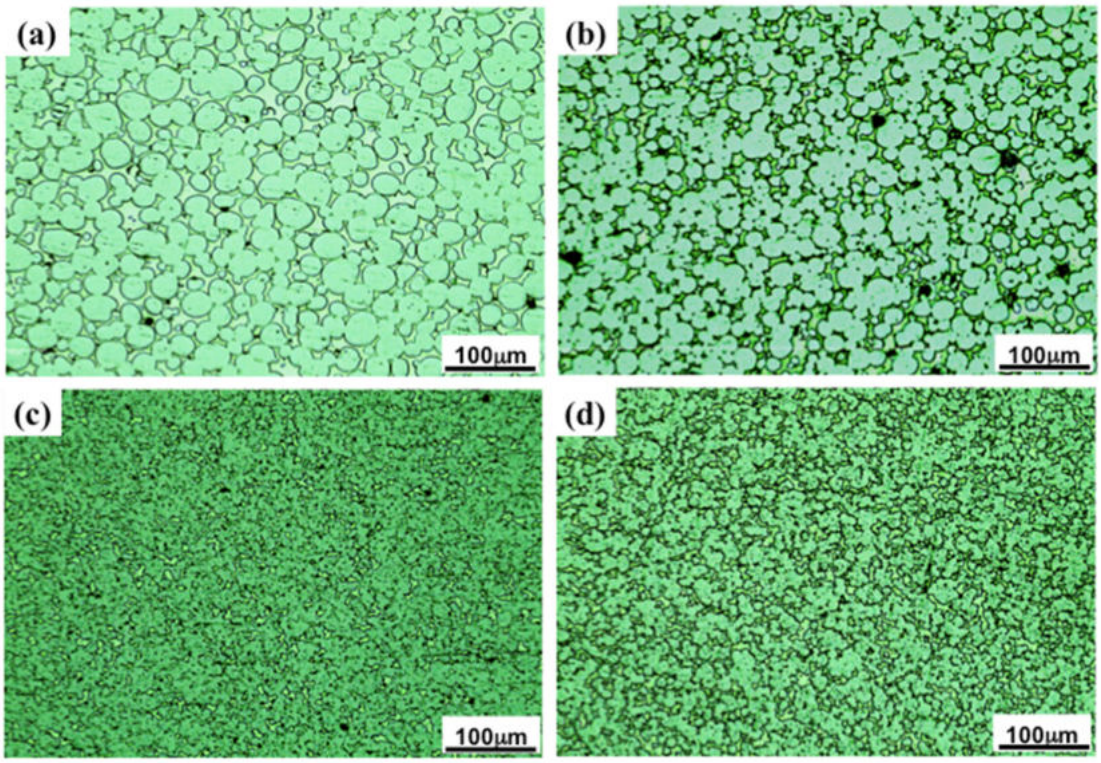

Figure 3. Optical microscope images of the sintered (**a**) W3Mo, (**b**) W12Mo, (**c**) W3Mo-YO, and (**d**) W12Mo-YO model alloys milled for 24 h.

3.2.2. SEM Observation

Figure 4 shows SEM images of the four different model alloys milled for 24 h. The effects of Mo contents without dispersed Y_2O_3 particles on the microstructures of the model alloys can be seen in Figure 4a,b. It demonstrates that the large spherical grain structure was observed in both W3Mo and W12Mo model alloys, suggesting that the dominant stage of liquid phase sintering has been identified. Furthermore, the model alloy with the higher amount of Mo tends to have a slightly smaller grain size. It has been proposed that increasing the Mo content from 3% and 12% resulted in a decrease in grain size, while the addition of excess Mo (20%) could result in the agglomeration and inhomogeneity of the grains [16].

Regarding with the formation of liquid phase sintering in the W3Mo and W12Mo model alloys, it should be noted that W and Mo are completely soluble in the solid and liquid stages, and therefore, the isomorphous system of W-Mo matrix was used for solid solution strengthening. The isomorphous W-Mo matrix without the effect of Y_2O_3 facilitates the process of liquid phase sintering. It has been reported that during liquid phase sintering, Mo dissolution acts in competition with W, resulting in a greatly refined W phase grain size [16].

On the other hand, Figure 4c,d shows the microstructure of the W3Mo-YO and W12Mo-YO model alloys. It can be seen clearly that fine grains and a homogeneous microstructure were obtained in both alloys, which tend to reflect solid state sintering. However, the increase of Mo content from 3 wt.% to 12 wt.% seems to not change the microstructure in the Y_2O_3 containing model alloys (Figure 4c,d). The small dark particles (about 1 μm) containing a high levels of W, Ni, Fe, Co, and O elements are distributed evenly within the tungsten matrix. It is believed that the presence of nano-Y_2O_3 oxides can interact with the solute elements during ball milling and form complex small oxide particles. Additionally, the dispersed Y_2O_3 particles could act as an inhibitor for diffusion of tungsten atoms at high temperature sintering, and thus, the abnormal or discontinuous grain growth of tungsten can be generated and facilitates the formation of a solid state during sintering [1,4]. Moreover, the γ-Ni(Fe,Co) binder phase has low activation energies and its diffusivity could be inhibited by Y_2O_3 oxide particles, thus creating a short diffusion path for solid state sintering.

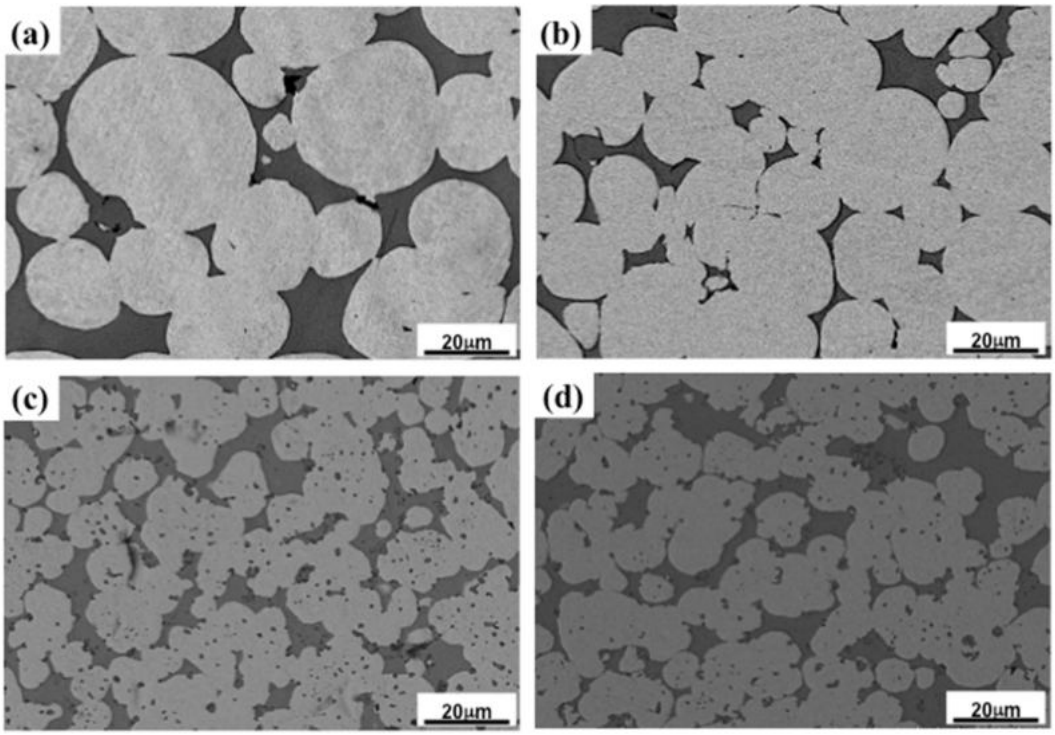

Figure 4. Scanning election microscope (SEM) images of the sintered (**a**) W3Mo, (**b**) W12Mo, (**c**) W3Mo-YO, and (**d**) W12Mo-YO model alloys milled for 24 h.

3.2.3. EDS Analysis

Figure 5 shows the results of EDS analyses of the different model alloys sintered after 24 h of milling. In Figure 5a,b, the W3Mo and W12Mo model alloys illustrate that the tungsten spherical grains appear as bright areas surrounded by the dark binder phase γ-Ni(Fe,Co). In this study, Mo formed a substitutional solid solution with tungsten grains, and thus, about 3 wt.% and 11 wt.% were detected from the tungsten matrix. It was found that the larger amounts of tungsten and molybdenum dissolved in the binder phase (totally, about 34 wt.%), suggesting a rapid diffusion route occurred during the liquid phase sintering. On the other hand, Figure 5c,d shows the model alloys with the addition of Y_2O_3 particles. A large number of the small dark particles was observed and uniformly distributed in the microstructure. The EDS results demonstrate that the presence of oxygen was detected in the particles, indicating the initial dispersed nano-Y_2O_3 reacts with alloying W, Fe, Ni, and Co elements to form large agglomerates. These particles can inhibit the movement of the grain boundary and diffusivity of W atoms at high temperature sintering and thus promote the formation of solid state during sintering. Meanwhile, EDS mapping was further performed on the model alloys. Figure 6 and Figure 7 show the EDS maps of W, Mo, Ni and Co elements in the W3Mo and W3Mo-YO samples, respectively. A high concentration of the Ni element can be seen clearly in the microstructure corresponding to the γ-Ni(Fe,Co) binder phase. Additionally, EDS mapping results indicate a uniform distribution of Mo element in the materials, suggesting a solid solution formed by mechanical alloying. However, the sub-micron size of the oxide-dispersed particles was not observed in the EDS maps (Figure 7) due to the limited resolution of EDS analysis.

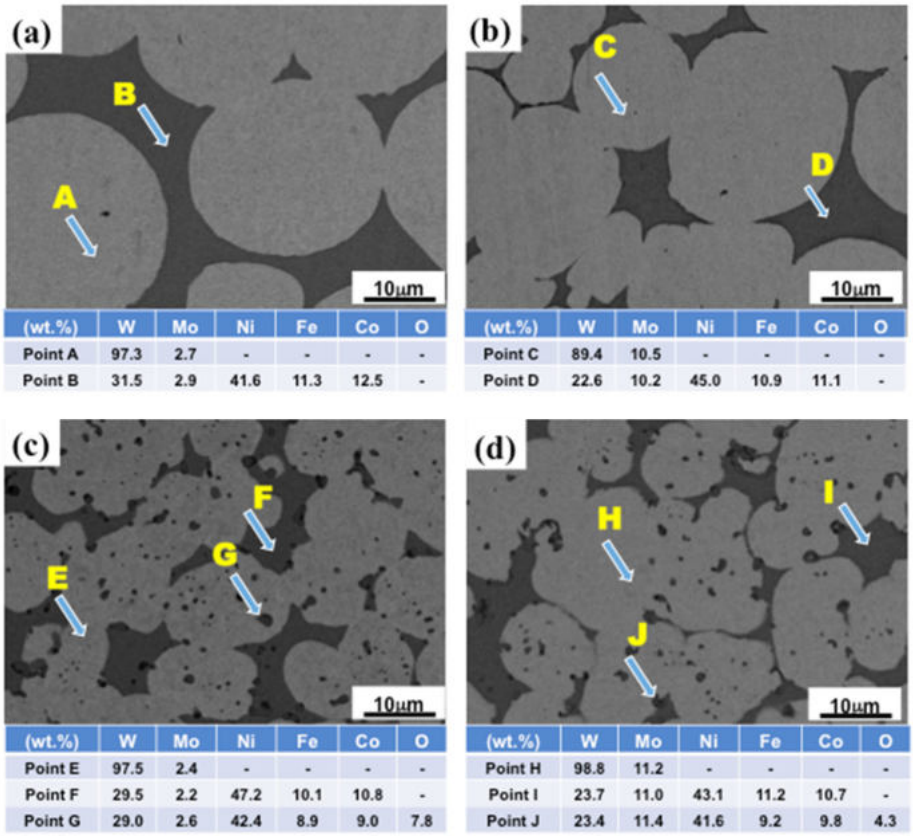

(wt.%)	W	Mo	Ni	Fe	Co	O
Point A	97.3	2.7	-	-	-	-
Point B	31.5	2.9	41.6	11.3	12.5	-

(wt.%)	W	Mo	Ni	Fe	Co	O
Point C	89.4	10.5	-	-	-	-
Point D	22.6	10.2	45.0	10.9	11.1	-

(wt.%)	W	Mo	Ni	Fe	Co	O
Point E	97.5	2.4	-	-	-	-
Point F	29.5	2.2	47.2	10.1	10.8	-
Point G	29.0	2.6	42.4	8.9	9.0	7.8

(wt.%)	W	Mo	Ni	Fe	Co	O
Point H	98.8	11.2	-	-	-	-
Point I	23.7	11.0	43.1	11.2	10.7	-
Point J	23.4	11.4	41.6	9.2	9.8	4.3

Figure 5. Energy-dispersive X-ray spectroscopy **(**EDS) analysis of the sintered (**a**) W3Mo, (**b**) W12Mo, (**c**) W3Mo-YO, and (**d**) W12Mo-YO model alloys milled for 24 h.

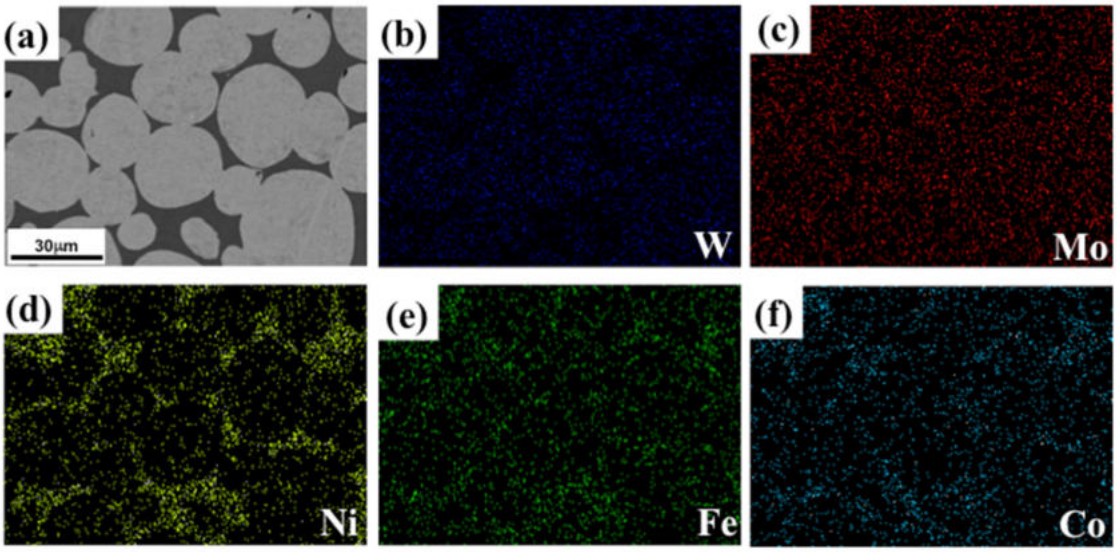

Figure 6. The EDS mapping of the W3Mo model alloy; (**a**) SEM image, (**b**) W map, (**c**) Mo map, (**d**) Ni map, (**e**) Fe map, and (**f**) Co map.

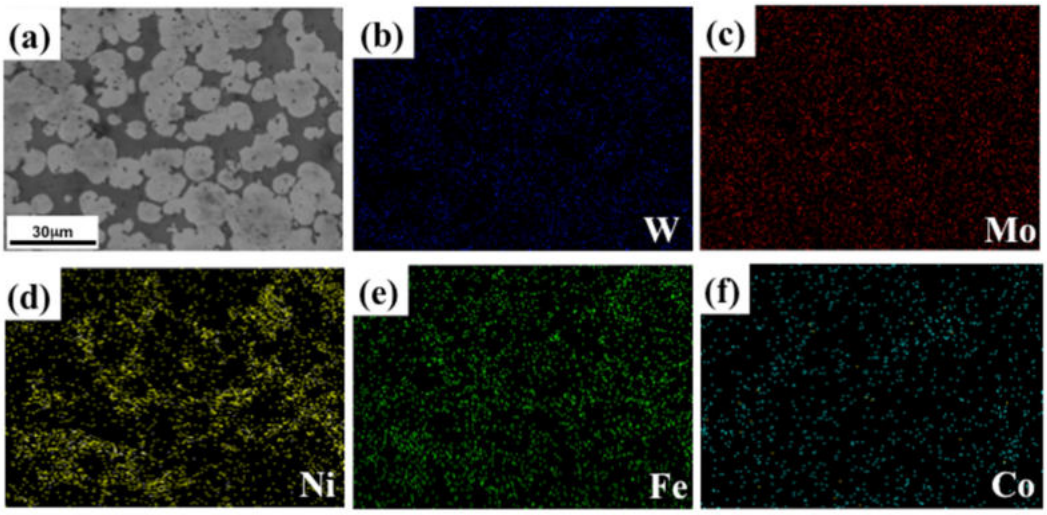

Figure 7. The EDS mapping of the W3Mo model alloy; (**a**) SEM image, (**b**) W map, (**c**) Mo map, (**d**) Ni map, (**e**) Fe map, and (**f**) Co map.

3.2.4. Relative Density

Table 2 lists the variation in relative densities of the different model alloys. It is clear that a higher relative densities were obtained from the model alloys dispersed with Y_2O_3 oxides, and the maximum value achieved was 96.56% for the W3Mo-YO sample. It is believed that Y_2O_3 oxides promote the formation of a solid state during sintering, which facilitated the grain refinement and homogeneous microstructure of tungsten alloys, and thus, relative density can be significantly increased. Additionally, it should be noted that a high Mo concentration can create a number of pores, thus reducing the densification of materials, as suggested in the W12Mo model alloy, which has the lowest relative density of 92.36%.

Table 2. The relative densities of the W-Mo-Ni-Fe-Co model alloys (%).

Model alloys	Relative Density (%)
W3Mo	93.02
W12Mo	92.36
W3Mo-YO	96.56
W12Mo-YO	94.13

3.3. Hardness and Nanoindentation

Figure 8 shows the variation of hardness as a function of milling time for the model alloys. The results demonstrate that the hardness increases with increasing milling time. The model alloys with added Y_2O_3 show a relatively high hardness of about 430 HV after 24 h milling, which is much greater than that of the Y_2O_3-free model alloys (about 355 HV). The change of hardness can be associated with solid to liquid phase transition during sintering. It has been widely reported that nano-oxide particles can act as the pinning points for dislocation motion and increase recrystallization temperature [8–12]. Therefore, it could be assumed that the presence of Y_2O_3 altered the sintering temperatures of the model alloys, which were varied within solid state, sub-solidus state, and liquid state range [12]. The high hardness of the W3M-YO and W12M-YO model alloys were subjected to solid phase sintering, providing a fine grain structure and homogeneous distribution of the binder phase. The addition Y_2O_3 particles could dominate for solid-state diffusivity, chemical reactivity, and coherent interfaces between tungsten matrix and binder phase during milling [17].

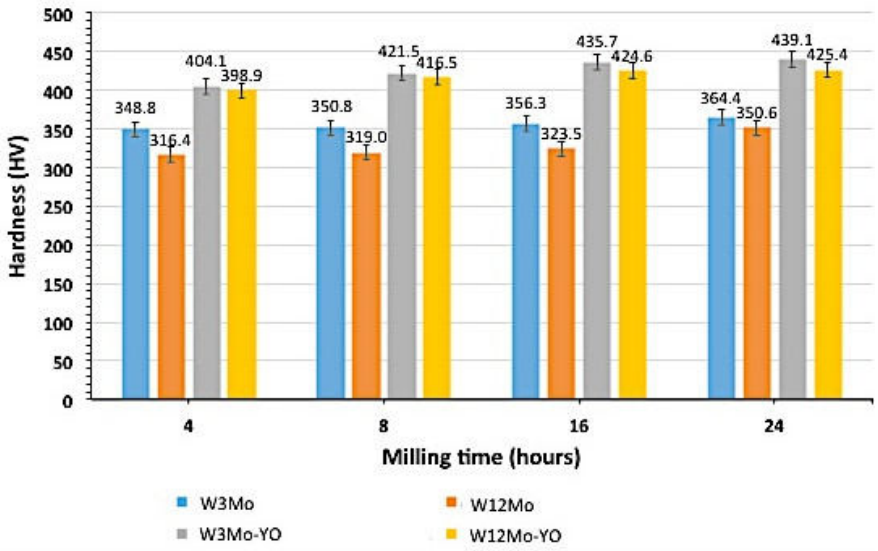

Figure 8. The microhardness of the model alloys at different durations of milling.

Nanoindentation was further used to determine the hardness and elastic modulus of the model alloys after 24 h of milling, as shown in Figure 9. The results demonstrate that the highest hardness and elastic modulus values of 10.14 and 427.7 GPa were found in the W3Mo-YO model alloy. However, the model alloys without the Y_2O_3 addition show lower hardness and elastic modulus values, particularly in the case of the W12Mo sample (H: 8.84 GPa; M: 348.2 GPa). It has a similar trend as in Vickers' hardness testing (Figure 8). The results suggest that the presence of Y_2O_3 dispersoids plays an important role in determining the sintering behavior of the model alloys, which leads to transition between the solid and liquid states during sintering. It can be concluded that the mechanical properties were strongly influenced by grain structure, densification, and microstructure homogeneity, which are related to sintering behavior. Figure 10 shows there are 12 indents on the microstructure of the W3Mo alloy sample, and a further investigation was made of the individual tungsten grain and binder phases observed at "Indent 6" and "Indent 10", as shown in Figure 10b,c. The tungsten matrix has a hardness of 11.98 GPa and elastic modulus of 510.3 GPa, which are high compared to that of the γ-Ni(Fe,Co) binder phase, with a hardness of 9.44 GPa and elastic modulus of 407.8 GPa. Note that the grain size and the distribution of the γ-Ni(Fe,Co) binder phase are important in determining the mechanical properties of the alloys.

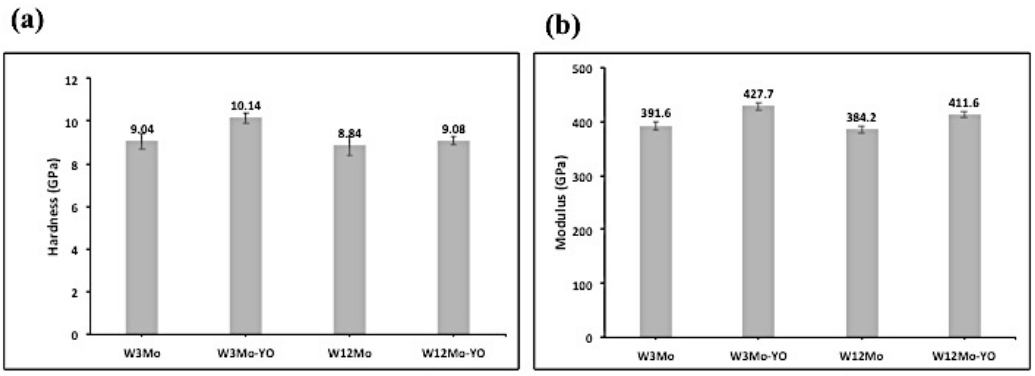

Model Alloys (Nanoindention)	Hardness (GPa)	Modulus (GPa)
W3Mo	9.04 ± 0.36	391.6 ± 7.78
W3Mo-YO	10.14 ± 0.27	427.7 ± 7.21
W12Mo	8.84 ± 0.46	384.2 ± 6.29
W12Mo-YO	9.08 ± 0.19	411.6 ± 5.48

Figure 9. Nanoindentation measurements of the hardness and elastic modulus of the model alloys.

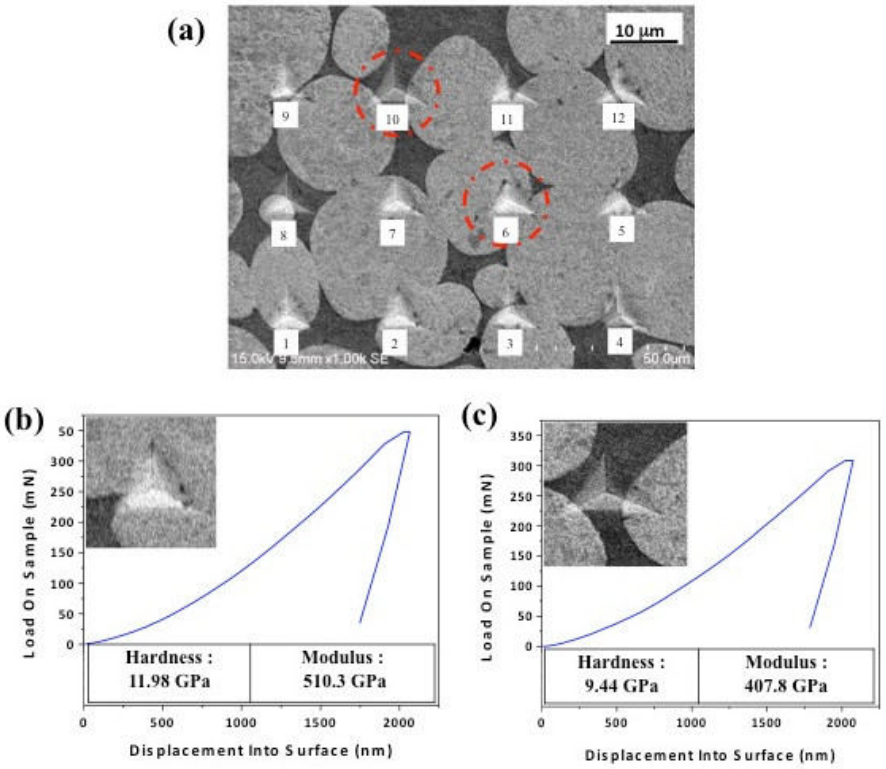

Figure 10. Nanoindentation measurements of the W3Mo model alloy; (**a**) SEM image of 12 indents and the load-displacement curve of (**b**) Indent "6" and (**c**) Indent "10".

4. Conclusions

In this study, W-Mo-Ni-Fe-Co model alloys dispersed with Y_2O_3 oxides were synthesized by mechanical alloying. The effects of Mo and oxide dipsersoids on characteristics and properties of the model alloys were investigated. The results show that the γ-Ni(Fe,Co) binder phase was formed after the pre-milling of Ni, Fe, and Co powders. The W-Mo matrix phase and γ-Ni(Fe,Co) binder were further milled by secondary ball milling. In W3Mo and W12Mo model alloys, the tungsten matrix, having a large spherical grain size and interconnected with the γ-Ni(Fe,Co) binder phase, was observed, suggesting the formation of a liquid state during sintering. On the other hand, the model alloys with added Y_2O_3 demonstrate grain refinement and uniform microstructure, suggesting solid phase sintering was achieved. The dispersed Y_2O_3 particles could act as inhibitors for diffusion of tungsten atoms and facilitate discontinuous grain growth of tungsten, promoting the formation of a solid state during sintering. Thus, it is believed that the addition of Y_2O_3 plays an important role in determining sintering behavior, which can influence the mechanical properties and densification of the model alloys.

Author Contributions: Conceptualization, C.C.; methodology, C.C.; formal analysis, C.C. and S.; investigation, S.; resources, C.C.; writing—original draft preparation, C.C.; writing—review and editing, C.C.; funding acquisition, C.C..

Funding: This research was funded by Ministry of Science and Technology (MOST) of Taiwan under the grant MOST 106-2221-E-259 -015 -MY2.

Conflicts of Interest: The authors declare no conflict of interest. The funders had no role in the design of the study; in the collection, analyses, or interpretation of data; in the writing of the manuscript, and in the decision to publish the results.

References

1. Lee, K.H.; Cha, S.I.; Ryu, H.J.; Hong, S.H. Effect of two-stage sintering process on microstructure and mechanical properties of ODS tungsten heavy alloy. *Mater. Sci. Eng. A* **2007**, *458*, 323–329.

2. Arora, A.; Rao, V.G. Tungsten Heavy Alloy for Defence Applications. *Mater. Technol.* **2004**, *19*, 210–215.
3. Lu, P.; German, R.M. Multiple grain growth events in liquid phase sintering. *J. Mater. Sci.* **2001**, *36*, 3385–3394.
4. German, R.M. Sintering Atmosphere Effects on the Ductility Sintering Atmosphere Effects on the Ductility of W-Ni-Fe Heavy Metals. *Metall. Trans. A* **2017**, *15*, 747–754.
5. Ryu, H.J.; Hong, S.H. Effects of sintering conditions on mechanical properties of mechanically alloyed tungsten heavy alloys. *Key Eng. Mater.* **2000**, *7*, 2–7.
6. Ryu, H.J.; Hong, S.H. Fabrication and properties of mechanically alloyed oxide-dispersed tungsten heavy alloys. *Mater. Sci. Eng. A* **2003**, *363*, 179–184.
7. Zhu, Y.B.; Wang, Y.; Zhang, X.Y.; Qin, G.W. W/NiFe phase interfacial characteristics of liquid-phase sintered W-Ni-Fe alloy. *Int. J. Refract. Met. Hard Mater.* **2007**, *25*, 275–279.
8. Chen, C.L.; Huang, C.L.; Zeng, Y. Synthesis of ODS heavy tungsten alloys through post-annealing and secondary ball milling. *Int. J. Refract. Met. Hard Mater.* **2015**, *48*, 359–364.
9. Chen, C.L.; Huang, C.L. Milling media and alloying effects on synthesis and characteristics of mechanically alloyed ODS heavy tungsten alloys. *Int. J. Refract. Met. Hard Mater.* **2014**, *44*, 19–26.
10. Chen, C.L.; Huang, C.L. The effects of alloying and milling on the formation of intermetallics in ODS tungsten heavy alloys. *Intermetallics* **2013**, *41*, 10–15.
11. Chen, C.L.; Ma, S.H. Study on characteristics and sintering behavior of W-Ni-Co tungsten heavy alloy by a secondary ball milling method. *J. Alloys Compd.* **2018**, *731*, 78–83.
12. Chen, C.L.; Ma, S.H. Effects of Ni/Co ratio and mechanical alloying on characteristics and sintering behavior of W-Ni-Co tungsten heavy alloys. *J. Alloys Compd.* **2017**, *711*, 488–494.
13. Bose, A.; German, R.M. Microstructural Refinement of W-Ni-Fe Heavy Alloys by Alloying Additions. *Metall. Trans. A* **1988**, *19*, 3100–3101.
14. Kemp, P.B.; German, R.M. Mechanical Properties of Molybdenum Alloyed Liquid Phase- Sintered Tungsten-Based Composites. *Metall. Trans. A* **1995**, *26*, 2187–2189.
15. Hamid, Z.A.; Moustafa, S.F.; Daoush, W.M.; Mouez, F.A.; Hassan, M. Fabrication and Characterization of Tungsten Heavy Alloys Using Chemical Reduction and Mechanical Alloying Methods. *Open J. Appl. Sci.* **2013**, *03*, 15–27.
16. Zhang, G.; Xiong, W.; Yang, Q.; Yao, Z.; Chen, S.; Chen, X. Effect of Mo addition on microstructure and mechanical properties of (Ti, W) C solid solution based cermets. *Int. J. Refract. Met. Hard Mater.* **2014**, *43*, 77–82.
17. Chen, C.L. Sutrisna Study of W-Co ODS coating on stainless steels by mechanical alloying. *Surf. Coat. Technol.* **2018**, *350*, 954–961.